Biochemical and Structural Characterization of the Cross-Linked Complex of Nitrogenase: Comparison to the ADP-AlF_4^--Stabilized Structure[†,‡]

Benedikt Schmid,[§] Oliver Einsle,[§,||] Hsiu-Ju Chiu,[§,⊥] Andreas Willing,[#,@] Mika Yoshida,[§,||] James B. Howard,[*,#] and Douglas C. Rees[*,§,||]

Division of Chemistry and Chemical Engineering 114-96, California Institute of Technology, Pasadena, California 91125, Howard Hughes Medical Institute, California Institute of Technology, Pasadena, California 91125, and Department of Biochemistry, University of Minnesota, Minneapolis, Minnesota 55455

Received August 15, 2002; Revised Manuscript Received October 27, 2002

ABSTRACT: The transient formation of a complex between the component Fe- and MoFe-proteins of nitrogenase represents a central event in the substrate reduction mechanism of this enzyme. Previously, we have isolated an *N*-[3-(dimethylamino)propyl]-*N*′-ethylcarbodiimide (EDC) cross-linked complex of these proteins stabilized by a covalent isopeptide linkage between Glu 112 and Lys β400 of the Fe-protein and MoFe-protein, respectively [Willing, A., et al. (1989) *J. Biol. Chem. 264*, 8499−8503; Willing, A., and Howard, J. B. (1990) *J. Biol. Chem. 265*, 6596−6599]. We report here the biochemical and structural characterization of the cross-linked complex to assess the mechanistic relevance of this species. Glycinamide inhibits the cross-linking reaction, and is found to be specifically incorporated into Glu 112 of the Fe-protein, without detectable modification of either of the neighboring residues (Glu 110 and Glu 111). This modified protein is still competent for substrate reduction, demonstrating that formation of the cross-linked complex is responsible for the enzymatic inactivation, and not the EDC reaction or the modification of the Fe-protein. Crystallographic analysis of the EDC-cross-linked complex at 3.2 Å resolution confirms the site of the isopeptide linkage. The nature of the protein surfaces around the cross-linking site suggests there is a strong electrostatic component to the formation of the complex, although the interface area between the component proteins is small. The binding footprints between proteins in the cross-linked complex are adjacent, but with little overlap, to those observed in the complex of the nitrogenase proteins stabilized by ADP-AlF_4^-. The results of these studies suggest that EDC cross-linking traps a nucleotide-independent precomplex of the nitrogenase proteins driven by complementary electrostatic interactions that subsequently rearranges in a nucleotide-dependent fashion to the electron transfer competent state observed in the ADP-AlF_4^- structure.

The mechanistic understanding of the nitrogenase reaction (reviewed in refs *1*−*5*) emphasizes two primary and interrelated processes: events involving reduction of substrates at the FeMo-cofactor center and electron transfer between the two protein components leading to substrate reduction, namely, electron transfer from the Fe-protein to the MoFe-protein. The electron transfer between the component proteins plays a central role in the overall mechanism due to the intricate timing of events likely regulated by ATP hydrolysis and associated Fe-protein conformational changes (*6*). The unique nature and importance of this step is exemplified by the observations that only the Fe-protein can serve as the electron donor leading to substrate reduction (other low-potential donors do not work) and that the nucleotide hydrolysis only occurs when both active protein components are present in a complex. In addition, the complex is short-lived, and its turnover, which must occur multiple times, is believed to represent the overall rate-determining step for substrate reduction (*7*, *8*).

In an attempt to better define the steps in the transfer of electrons from the Fe-protein to the MoFe-protein, including the role of nucleotide hydrolysis in this process, we have endeavored to trap the protein complex in various stages of turnover and to analyze the resulting species both biochemically and crystallographically. The first complex so studied was formed by stabilization of a putative transition state of ATP hydrolysis through the substitution of the aluminum

[†] This work was supported in part by NIH Grant GM45062 and a Deutsche Forschungsgemeinschaft research fellowship (B.S.). Portions of this research were carried out at the Stanford Synchrotron Radiation Laboratory (SSRL), a national user facility operated by Stanford University on behalf of the U.S. Department of Energy (DOE), Office of Basic Energy Sciences. The SSRL Structural Molecular Biology Program is supported by the DOE, Office of Biological and Environmental Research, and by the NIH, National Center for Research Resources, Biomedical Technology Program, and the National Institute of General Medical Sciences.

[‡] The Protein Data Bank codes for the coordinates of the EDC-cross-linked and high-resolution ADP-AlF_4^--stabilized complexes of the nitrogenase proteins are 1M1Y and 1M34, respectively.

* To whom correspondence should be addressed. E-mail: (J.B.H.) howar001@umn.edu; (D.C.R.) dcrees@caltech.edu. Telephone: (626) 395-8393. Fax: (626) 744-9524.

[§] Division of Chemistry and Chemical Engineering 114-96, California Institute of Technology.

[||] Howard Hughes Medical Institute; California Institute of Technology.

[⊥] Present address: Structural Biology, Tularik Inc., South San Francisco, CA 94080.

[#] University of Minnesota.

[@] Present address: Cognis Deutschland GmbH Co. KG, D-40551 Düsseldorf, Germany.

10.1021/bi026642b CCC: $22.00
Published on Web 12/04/2002

tetrafluoridate anion (AlF_4^-) for the terminal, leaving phosphate during enzymic turnover (*9*, *10*). The structure of this ADP-AlF_4^--stabilized nitrogenase complex (*11*) provided a strong rationale for the mechanism of nucleotide hydrolysis and for the initial electron transfer from the [4Fe-4S] cluster of the Fe-protein to the [8Fe-7S] cluster (the P-cluster) of the MoFe-protein. The mode of nucleotide binding and transition state stabilization by the Fe-protein component of the nitrogenase complex was similar to that observed in the larger family of nucleotide-dependent regulatory proteins, e.g., G-proteins, *ras*, and transducin (see ref *12*). Although these similarities were anticipated from the structural resemblance of the Fe-protein core to the G-protein family consensus sequences and structure (*13*−*15*), the ADP-AlF_4^--stabilized nitrogenase complex revealed several unexpected results. Most significantly, the nucleotide hydrolysis intermediate was stabilized by amino acid side chains *across* the interface of the Fe-protein homodimer and well away from the Fe-protein−MoFe-protein interface. Hence, the MoFe-protein appears more as a template to stabilize the Fe-protein conformation during hydrolysis and does not directly participate in hydrolysis. In this nucleotide-stabilized transition state, the electron donor and acceptor in the two-protein complex are significantly closer than in a complex obtained by van der Waals contact docking of the native proteins. The required role of the nucleotide hydrolysis in turnover was further demonstrated by an analysis of the complex of the native MoFe-protein and an Fe-protein variant with a deletion of Leu 127 near the terminal phosphate binding site (*16*). This altered Fe-protein readily formed a tight complex with the MoFe-protein even in the absence of nucleotide; however, the structure of this complex (*17*) demonstrated that precise alignments of the Fe-protein side chains at the subunit interface were not possible, and therefore, nucleotide could not bind in the same detailed orientation needed for hydrolysis.

A number of years ago, we reported the formation of a different complex between the Fe-protein and MoFe-protein, one that was stabilized by a highly specific isopeptide cross-link generated using the water soluble carbodiimide *N*-[3-(dimethylamino)propyl]-*N*′-ethylcarbodiimide (EDC)[1] as the mediator (*18*, *19*). The reaction had properties expected of a potentially mechanistically relevant complex; namely, the cross-linking was rapid, was dependent upon protein component ratio and concentrations, and was inhibited by NaCl in a pattern similar to the inhibition of substrate reduction. However, this complex did not require nucleotide, and its formation led to the inactivation of nitrogenase for substrate reduction. Most striking was the specificity of the reaction; only Glu 112 from one of the two Fe-protein subunits and Lys 400 of the MoFe-protein β-subunit were cross-linked, even though these residues are surrounded by numerous other charged residues that could potentially participate in this process. To better understand how the cross-linked complex might be related to the ADP-AlF_4^--stabilized complex, we have undertaken new studies characterizing the specificity of the EDC reactive site and have determined the three-dimensional structure of the cross-linked complex by X-ray crystallography at 3.2 Å resolution. Further, we have extended the resolution of the ADP-AlF_4^--stabilized complex structure to 2.3 Å resolution. These studies confirm that a highly specific chemical cross-link is formed by the EDC reaction and indicate that the cross-linked complex, although potentially related, is not equivalent to the putative electron transfer complex.

[1] Abbreviations: Av1, MoFe-protein from *Azotobacter vinelandii*; Av2, Fe-protein from *A. vinelandii*; EDC, *N*-[3-(dimethylamino)propyl]-*N*′-ethylcarbodiimide; MPD, 2-methyl-2,4-pentanediol.

MATERIALS AND METHODS

Av2 (Fe-protein from *Azotobacter vinelandii*) and Av1 (MoFe-protein from *A. vinelandii*) were purified and analyzed as previously described (*20*) using anaerobic conditions throughout. The specific activity at pH 8.0 and 30 °C for Av1 was 2050−2200 nmol of acetylene reduced min^{-1} (mg of protein)$^{-1}$ and for Av2 2800−3100 nmol of acetylene reduced min^{-1} (mg of protein)$^{-1}$. Both the EDC-mediated cross-linked complex (*19*) and the ADP-AlF_4^--stabilized complex (*9*) were prepared as described previously using an ∼6-fold excess of Av2 over Av1 to ensure complete conversion of the Av1 to the respective complex. This ratio favors complete complex formation based upon the Av1 component, which facilitates isolation of the complex by chromatography on a Superdex S-200 sizing column. Because the ADP-AlF_4^--stabilized complex was formed under normal enzymic turnover conditions, creatine phosphate (10 mM) and phosphocreatine kinase (0.1 mg/mL) were also present in the complex formation reaction mixture.

[2-^{14}C]Glycinamide was prepared (98.5% yield) by a "single-pot" protocol of esterification, followed by aminolysis using 50 μmol of [2-^{14}C]glycine (250 μCi, New England Nuclear). The specific radioactivity of the amide was determined to be 11 847 dpm/nmol by quantitative amino acid analysis and scintillation counting. [2-^{14}C]Glycinamide-modified Av2 was carboxymethylated by alkylation with 3-[^{3}H]iodoacetic acid and digested with trypsin (*21*). The peptides were isolated using HPLC ion exchange and C-4 reverse phase columns and the sequences determined by Edman degradation. The radioactivity was quantified for each cycle of repetitive Edman degradation after identification of individual PTH amino acids (*19*, *21*).

Both the cross-linked and ADP-AlF_4^--stabilized complexes were crystallized under anaerobic conditions using the microcapillary batch method (*14*) from a mixture containing 15 μL of complex and 20 μL of precipitant. For the cross-linked complex, the protein solution consisted of 33 mg/mL protein, 40 mM Tris-HCl (pH 8.0), 200 mM NaCl, 20% (v/v) 2-methyl-2,4-pentanediol (MPD), and 5 mM $Na_2S_2O_4$, while the precipitant contained 75 mM Tris-HCl (pH 8.0), 510 mM cadaverine HCl, 20.9% (w/w) PEG 6000, and 2 mM $Na_2S_2O_4$. These crystallizations were conducted at 4 °C. Isomorphous crystals could be prepared with lower concentrations or even in the absence of cadaverine, but the diffraction quality was significantly poorer. For the ADP-AlF_4^--stabilized complex, the protein solution consisted of 15 mg/mL protein, 100 mM MOPS/Tris base (pH 7.3), 100 mM NaCl, 5 mM NaF/0.25 mM $AlCl_3$, 1 mM $MgCl_2$, 1 mM Na_2ATP, and 5 mM $Na_2S_2O_4$, while the precipitant contained 100 mM cacodylate-HCl buffer (pH 6.5), 30 mM $MgCl_2$, and 19% (w/w) PEG 8000. Both complexes crystallized with two $\alpha_2\beta_2\gamma_4$ species in the asymmetric unit. The cross-linked complex crystallized in space group $P2_12_12_1$ with the

Table 1: Data and Refinement Statistics

	cross-link	ADP-AlF_4^-
data collection statistics		
resolution range (Å)	50−3.2	20−2.3
no. of total observations	225603	665961
no. of unique observations	105200	273781
completeness (%)[a]	81.1 (70.3)	83.3 (66.9)
R_{merge} (%)[a,b]	8.5 (66.6)	12.8 (26.6)
refinement statistics		
resolution range (Å)	50−3.2	20−2.3
R (%)[c]	27.9	20.0
R_{free} (%)[d]	33.0	23.6
rms deviations from ideal values		
bond lengths (Å)	0.021	0.012
bond angles (deg)	1.44	1.63
Ramachandran statistics (%)[e]		
most favored	77.4	89.9
additionally allowed	21.1	9.9
generously allowed	1.5	0.2
disallowed	0.0	0.0

[a] Values in parentheses correspond to the highest-resolution shell. [b] $R_{merge} = \sum_{hkl,I}(\sum_I|I_{hkl,I} - \langle I_{hkl}\rangle|)/(\sum_{hkl,I}\langle I_{hkl}\rangle)$, where I_{hkl} is the intensity of an individual measurement of the reflection with indices *hkl* and $\langle I_{hkl}\rangle$ is the mean intensity of that reflection. [c] $R = (\sum_{hkl}||F_o| - |F_c||)/(\sum_{hkl}|F_c|)$. [d] $R_{free} = R$ defined for 5% of the reflections excluded from the refinement. [e] The most favored, additionally allowed, generously allowed, and disallowed regions are defined by PROCHECK (*38*).

following cell dimensions: $a = 113.3$ Å, $b = 214.9$ Å, and $c = 320.5$ Å. The ADP-AlF_4^--stabilized complex crystallized in space group $C2$ with the following cell dimensions: $a = 326.1$ Å, $b = 75.8$ Å, $c = 312.2$ Å, and $\beta = 102.6°$. For cryocrystallography, the crystals were successively transferred into solutions with increasing concentrations of MPD up to 20% (v/v). Diffraction data were collected at the Stanford Synchrotron Radiation Laboratory from single crystals of each complex at −180° on beamline 9-2 ($\lambda = 1.005$ Å). The data were processed using DENZO and SCALEPACK (*22*), and the statistics are summarized in Table 1.

The structures of each complex were determined by molecular replacement with the program AMORE (*23*) using the MoFe-protein and the Av1−Av2(ADP-AlF_4^-) structures (PDB entries 3MIN and 1N2C, respectively) as search models. The models were refined by cycles of rigid body optimization, conjugate gradient minimization, simulated annealing, and individual *B*-factor refinement using the program CNS (*24*). A bulk solvent correction and an anisotropic *B*-factor scaling were applied to the reflection data. Initially, tight noncrystallographic symmetry restraints (500 kcal mol^{-1} $Å^{-2}$) were applied to the equivalent halves of the complex and to the two equivalent complexes, and then gradually released at the latter stages of refinement. For the cross-linked complex, the final model contains two $\alpha_2\beta_2\gamma_4$ complexes, where each complex contains one Av1 molecule with two α-subunits (residues 4−481) and two β-subunits (residues 2−523), two Av2 dimers, each with two γ-subunits (residues 1−274), two FeMo-cofactors, two P-clusters, and two [4Fe-4S] clusters, while the final model of the ADP-AlF_4^--stabilized complex contains two complexes, with each complex consisting of one Av1 tetramer with two α-subunits (residues 4−481) and two β-subunits (residues 2−523), two Av2 dimers, each with two γ-subunits (residues 1−274), two FeMo-cofactors, two P-clusters [in the reduced P^N state (*25*)], two [4Fe-4S] clusters, four MgADP-AlF_4^- molecules, and 1588 water molecules. The final R was 27.9% ($R_{free} = 33.0\%$) for all the data between 50 and 3.2 Å for the cross-linked complex, while the final R for the ADP-AlF_4^--stabilized complex was 20.0% ($R_{free} = 23.6\%$) for all the data between 20 and 2.3 Å. A more complete listing of refinement statistics is given in Table 1. Although the R factors are relatively high for the cross-linked complex, given the moderate resolution, data quality, and the disorder apparent in two of the four Av2 dimers away from the cross-linking site, the refinement was deemed appropriate for characterizing the mode of interaction between the cross-linked nitrogenase proteins.

Unless otherwise noted, PDB entries 2NIP (for the native, nucleotide-free Fe-protein) and 3MIN (for the native MoFe-protein) were used in comparisons to the relevant conformations in the complexes.

RESULTS AND DISCUSSION

Chemical cross-linking of Av2 to Av1 through the EDC-mediated formation of an isopeptide bond is remarkably specific for both protein components, with only a single residue in each protein modified (*18*, *19*), yet the origin of the specificity is not obvious since neither is a conserved residue. To better understand the molecular specificity and the relevance, if any, of the cross-linked complex to the enzyme turnover cycle, we have determined the three-dimensional structure by X-ray crystallography to 3.2 Å resolution. In addition, another well-defined complex of the nitrogenase components, the ADP-AlF_4^--stabilized complex (*11*), is now extended to higher resolution (2.3 Å). These structures are shown in Figure 1. As anticipated from the biochemical characterizations, in the cross-linked complex, two Av2 dimers are bound to each Av1 tetramer through an isopeptide linkage between Glu 112 of Av2 and Lys β400 of Av1 (Figure 2). At the resolution of this analysis, the conformations of the two crystallographically independent Av1 tetramers are essentially unchanged from the structure of free Av1, with average rms deviations in Cα positions of 0.4 Å. The conformations of the eight crystallographically independent Av2 subunits are also similar to the subunits of native Av2, with average rms deviations in Cα positions of 0.5 Å. However, the relative orientation of the subunits within an Av2 dimer for the cross-linked and native states showed some differences as reflected in the somewhat larger rms deviations in the Cα positions (0.7 Å). Comparisons of these conformations indicate that the Av2 dimer in the cross-linked complex has a more open structure than in the native Av2 dimer, corresponding to an *increase* in the hinge angle between the subunits of ∼4°. Most importantly, this change is substantially different from the *decrease* of ∼25° in the hinge angle observed for Av2 in the ADP-AlF_4^--stabilized complex (*11*).

As shown in Figure 1 and in more detail in Figure 3, the mode of Av2 binding to Av1 is significantly different in the EDC-cross-linked complex than in the ADP-AlF_4^--stabilized complex. For the ADP-AlF_4^--stabilized complex, the 2-fold symmetry axis of the Av2 dimer is nearly coincident with the pseudo-2-fold axis between the α- and β-subunits of Av1 that passes through the P-cluster. Notably, in this complex there is an extensive binding interface between Av1 and Av2

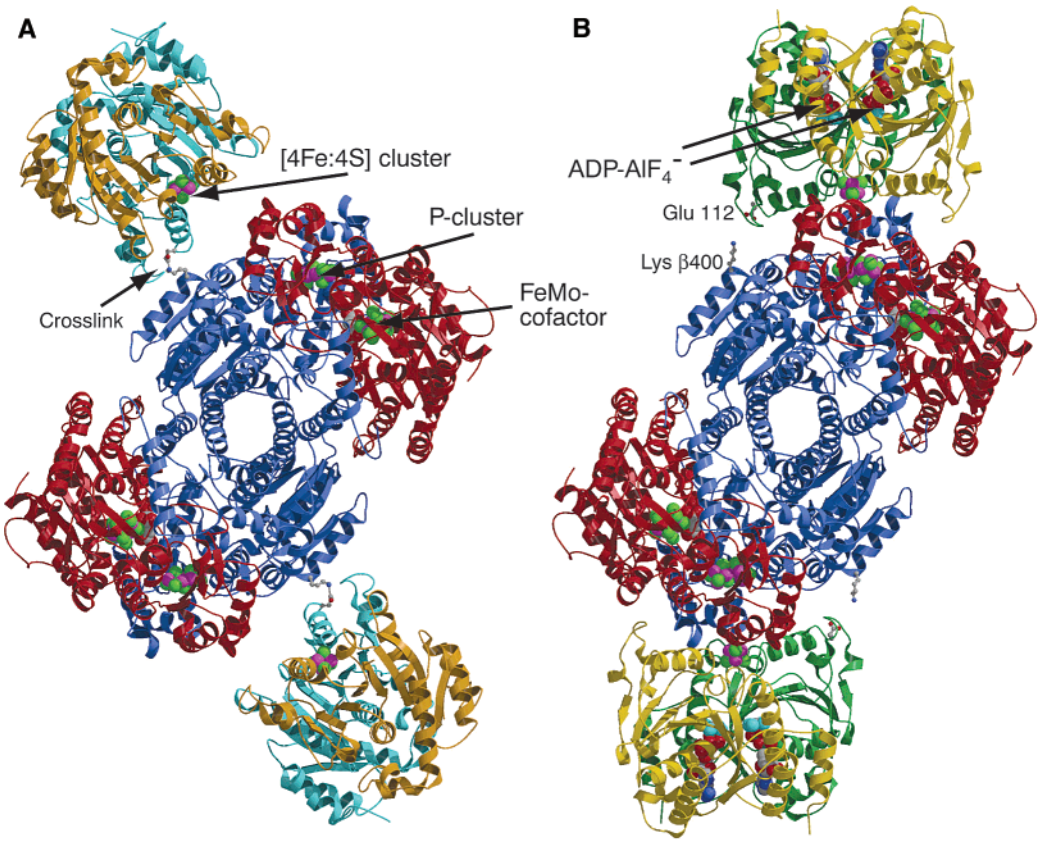

FIGURE 1: Ribbon diagrams of the $\alpha_2\beta_2\gamma_4$ complexes between the nitrogenase component proteins Av1 and Av2, stabilized by (A) the EDC-mediated cross-link between Glu 112 and Lys β400 and (B) ADP-AlF_4^-. The view is down the 2-fold axis that relates each set of $\alpha\beta\gamma_2$ subunits to the other. The MoFe-protein α-subunits are in red; the β-subunits are in blue, and the individual γ-subunits of each Fe-protein are in orange and cyan for the cross-linked complex and in yellow and green in the ADP-AlF_4^--stabilized complex. The residues participating in the cross-link in panel A are depicted in ball-and-stick mode. The cofactors and nucleotides are represented with space-filling models, color-coded by atoms with Fe in purple, S in green ([4Fe-4S] cluster, P-cluster, and FeMo-cofactor; the Mo atom is not visible), O in red, and C in gray (homocitrate, ADP) as well as N in blue and F in cyan (ADP-AlF_4^-; P, Al, and Mg atoms not visible). This figure was prepared with Molscript (*39*) and Raster3D (*40*).

that involves both subunits of Av1 and both subunits of Av2. In striking contrast, Av2 in the cross-linked complex binds adjacent to the surface of Av1 utilized in the ADP-AlF_4^- complex, the interactions between components are far less extensive, and the interaction site involves only the β-subunit of Av1 and one of the two Av2 subunits. The orientations of Av2 with respect to Av1 also differ substantially in the two complexes, as indicated by the ~45° difference between the directions of the Av2 2-fold axes in these structures.

The specificity of the EDC cross-link between Av1 and Av2 is all the more remarkable when it is considered in the context of the complex structure (Figures 1A and 4). When the region of Av1 around Lys β400 is examined, there are other lysine residues, e.g., residues β302, β303, β403, β404, β417, and β425, that might have been within reach of an activated Glu 112, yet none are observed by either chemical analysis or the X-ray structure to form an isopeptide bond with Av2. Even more impressive is the number of Av2 carboxylic acids in the environment of Glu 112. Indeed, Glu 112 is part of a pocket or patch containing multiple carboxylic acids, including Glu 68, 71, 73, 110, 111, 112, and 116 and Asp 69. As indicated by the electrostatic surfaces of the two proteins (Figure 4), the cross-linked residues are positioned among the most highly and complementary charged regions of Av1 and Av2. Consequently, although neither Glu 112 nor Lys β400 is conserved among the nitrogenase protein sequences, these patches of charges are conserved, and it may be that the overall electrostatic interaction between these two sites dominates the protein−protein interactions reflected in the cross-linking process.

Perhaps the most unexpected feature of the cross-linked complex structure is the relatively few contacts between Av1 and Av2, other than in the immediate vicinity of the cross-linking isopeptide. In addition to Lys β400 and Glu 112, the principal contributions (surface area of >10 Å^2) to the binding interface are provided by residues Glu β60, Lys β403, Lys β404, and Ile β423 of Av1 and Glu 68, Asp 69, Glu 71, Ile 103, and Glu 111 of Av2. The protein surfaces around the Av2 [4Fe-4S] cluster and the P-cluster of Av1 remain accessible to solvent, consistent with the conclusions of previous spectroscopic studies (*26*). Of potential significance, Asp 69 is positioned near Lys β400 in both the cross-linked and ADP-AlF_4^--stabilized complexes, and actually forms a salt bridge to this lysine in the latter complex. The paucity of contacts in the cross-linked complex is underscored by a comparison of the amount of surface area buried by Av2 on Av1 in the two complexes. In contrast to the area of ~3600 Å^2 of the Av1 and Av2 surfaces buried at the interface in the ADP-AlF_4^- complex, only ~500 Å^2 is covered in the corresponding interface of the cross-linked complex, which is less than the surface area typically buried in crystal lattice contacts [~800 Å^2 (*27*)]. This small interaction area also likely allows the variability that is apparent in the orientation of Av2 with respect to Av1

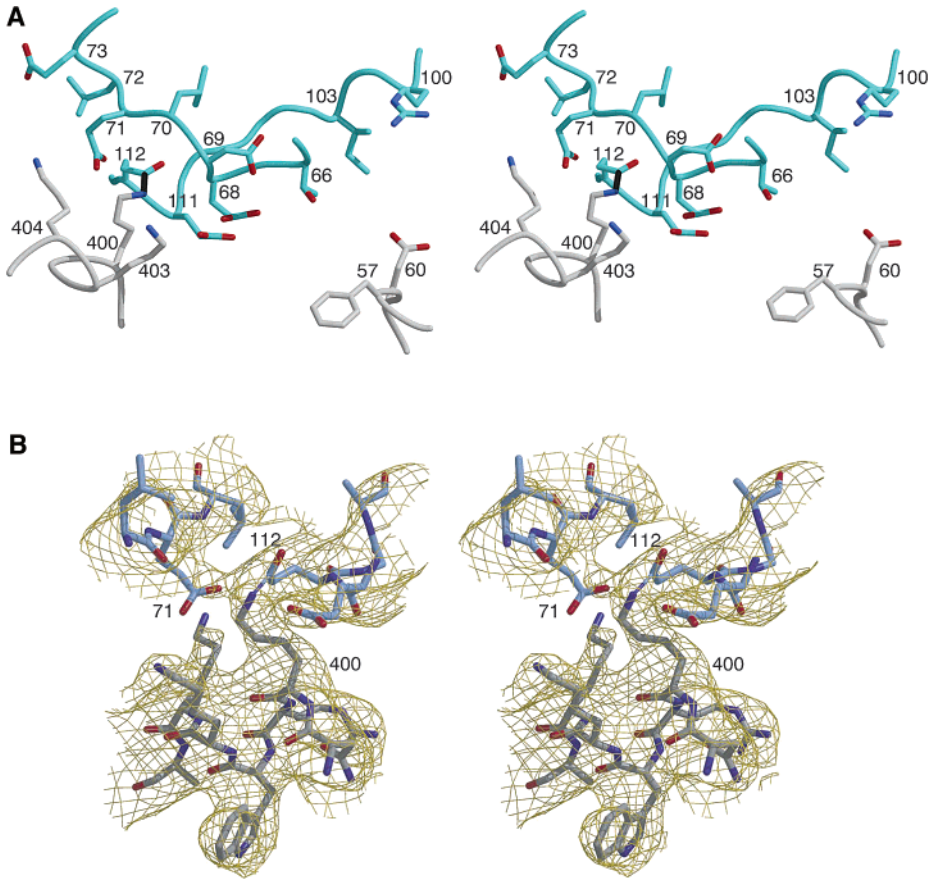

FIGURE 2: Stereoviews of the region surrounding the isopeptide linkage between Glu 112 of Av2 and Lys β400 of Av1. (A) Structure of the interacting residues, with Av2 and the Av1 β-subunit shown in cyan and gray, respectively, with N and O atoms depicted in blue and red, respectively. The significant number of potentially cross-linkable residues in this region is evident. (B) Electron density map surrounding the isopeptide linkage, calculated from the final, averaged $2F_o - F_c$ map, and contoured at one standard deviation. Although the residues are not sufficiently close to form a cross-link, the proximity of Av2 residue Glu 71 to Lys β400 in the cross-linking site is evident. This figure was prepared with Molscript (*39*) and Raster3D (*40*).

(Figure 3A). In addition to the isopeptide linkage, the mode of binding between Av2 and Av1 observed in the crystal appears to be stabilized by crystal lattice contacts (with ~600 Å^2 buried) to a second, non-cross-linked Av1; it should be noted that all four Av2 subunits in the unit cell exhibit similar crystal packing interactions with an adjacent Av1. Hence, the observed orientation of the Av2 dimer may be determined as much by the crystal lattice as by interactions with its partner Av1.

The electrostatic potential surfaces of the two components shown in Figure 4 suggest that other proteins with strongly acidic or basic patches might also interact or cross-link. However, even under conditions more vigorous than those leading to rapid and quantitative cross-linking between Av1 and Av2, we have not been able to detect cross-linking between either component and other proteins. For example, highly positively charged small proteins such as ribonuclease or cytochrome *c* or acidic proteins such as insulin, flavodoxin, or ferredoxin (the latter two are known electron donors for nitrogenase turnover in vivo) were not cross-linked to Av1 or Av2 (data not presented). These results strongly suggest that the specificity observed for Av1−Av2 cross-linking arises, at least in part, from a prerequisite noncovalent complex of the two components.

Nevertheless, in principle, other nucleophiles or acids should participate in the EDC reaction. Carbodiimides have long been exploited for both general and site specific carboxyl modification of proteins, including a method for determining the number of free carboxyl groups in a protein (*28*). In contrast to the absence of reaction with small proteins, nitrogenase reacts with glycinamide, a small molecule nucleophile, at modest concentrations, and the reaction substantially inhibits the protein cross-linking of Av1 and Av2 (Figure 5). When the reaction included [2-^{14}C]-glycinamide, the radiolabel was >95% in Av2 (top bar graph, Figure 5), which is consistent with the results for Av1−Av2 cross-linking where the carboxylate portion of the unique isopeptide bond was exclusively from Av2 (*19*). Furthermore, Av2, but not Av1, was labeled with [2-^{14}C]glycinamide in the EDC-mediated reaction with the individual component proteins (not shown). After the reaction, Av1 fully retained the capacity to cross-link with virgin Av2, while Av2 modified by the glycinamide could no longer cross-link to Av1 (Figure 5, lanes C and D). These results suggest a direct correlation between the site of glycinamide incorporation and the site of protein cross-linking.

The glycinamide inhibition of cross-linking was not due to random blocking of acidic groups, however, but rather was highly specific. Using trypsin-digested Av2 modified with [2-^{14}C]glycinamide (0.92 mol/mol of subunit), a single labeled peptide was observed by ion exchange FPLC. The single ^{14}C-labeled peak (chromatogram not shown) coincided with the cysteinyl-containing tryptic peptide previously determined to be residues 101−140 of Av2 (*21*). Amino acid

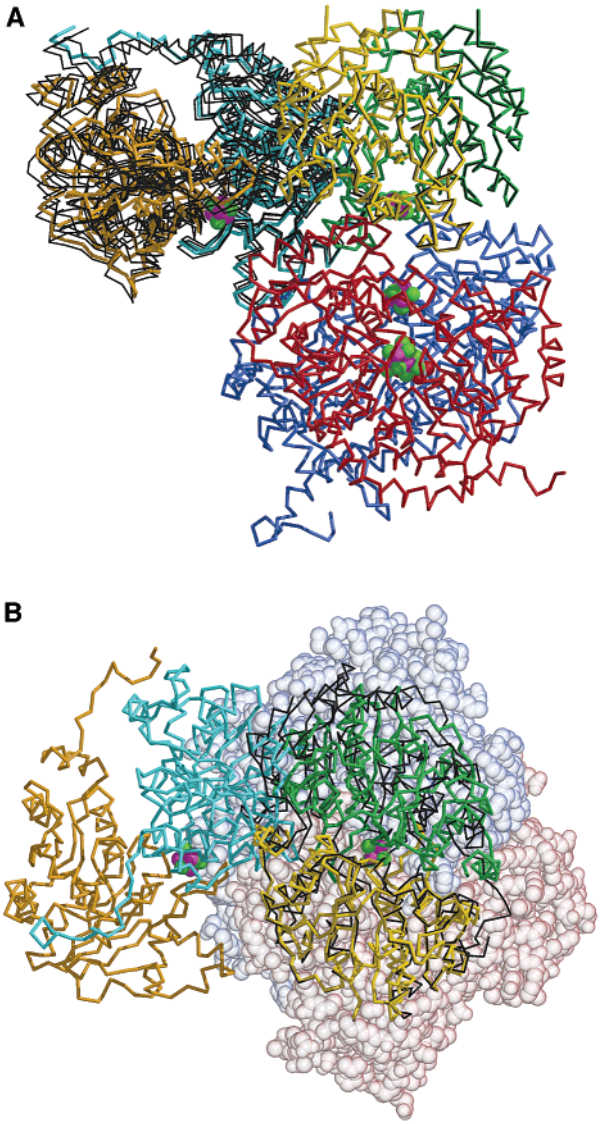

FIGURE 3: Relationship between the modes of binding of Av2 to Av1 in the cross-linked and ADP-AlF_4^--stabilized complexes. (A) Cα trace indicating the positions of the Av2 subunits in a given complex relative to a fixed orientation of the associated αβ subunit pair of Av1. The four crystallographically independent copies of Av2 bound to Av1 in the cross-linked complex (left side) are depicted in either cyan and orange (for the Av2 subunit illustrated in Figure 1A) or black for the remaining subunits. Crystallographically independent copies of Av2 bound to Av1 in the ADP-AlF_4^--stabilized complex are depicted in either yellow and green (for the Av1 subunit illustrated in Figure 1B) or black for the remaining subunits. The significantly greater variability in binding position between Av2 and Av1 in the cross-linked complex relative to the ADP-AlF_4^--stabilized complex is evident. The orientation of this figure is perpendicular to the 2-fold axis relating subunits in the Av1 αβ-dimer and in the Av2 dimer of the ADP-AlF_4^--stabilized complex. The cofactors are colored as in Figure 1B. (B) Alternate representation of the same interactions, now viewed down the 2-fold axis relating subunits in the Av1 αβ-dimer. Only one of the crystallographically independent Av2 dimers is illustrated for the cross-linked and ADP-AlF_4^--stabilized complexes. The Av1 α- and β-subunits are shown as a CPK model, shaded light red and blue, respectively. The nearly nonoverlapping, but adjacent, binding surfaces between Av2 and Av1 in these two complexes are apparent. Black lines designate the position of the native, nucleotide-free Av2 in a hypothetical complex with Av1, following superposition onto the subunit of the ADP-AlF_4^--stabilized complex interacting with the Av1 α-subunit. This figure was prepared with Molscript (*39*) and Raster3D (*40*).

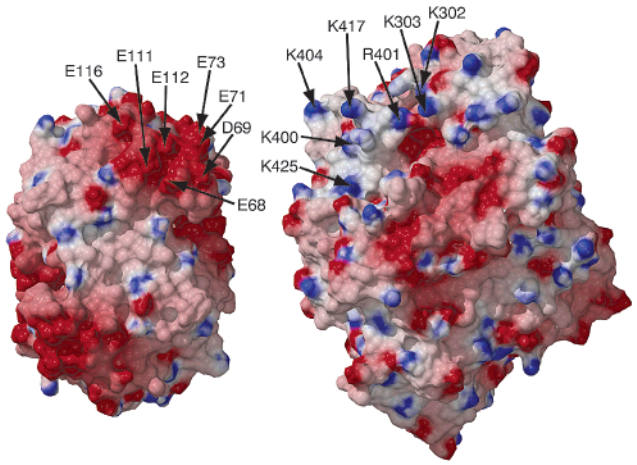

FIGURE 4: Electrostatic potential surface for Av1 and Av2, highlighting the residues involved in the cross-linking interaction. Av1 is shown in approximately the same orientation as Figure 3B, while Av2 is viewed down the dimer 2-fold axis, illustrating the surface that interacts with Av1. The complementary nature of the electrostatic surfaces in this region may been seen, with the locations of various charged residues indicated. Negative and positive potentials are shown in red (−15*kT*) and blue (15*kT*), respectively. This figure was prepared with DELPHI (*41*), MSMS (*42*), DINO (www.dino3d.org), and Raster3D (*40*).

analysis and Edman degradation confirmed the identification of this peptide, and Edman degradation of four peptides derived from chymotryptic digestion of the peptide found the radioactivity only in the Edman degradation cycle corresponding to Glu 112 of the Av2 sequence. It is important to note that two of the peptides from the chymotryptic digestion begin with Glu 110, yet only the PTH amino acid from the Glu 112 cycle was radioactive, with no evidence for derivatization of either Glu 110 and Glu 111; under these experimental conditions, even low-level, partial modification of residues 110 and 111 would have been easily detected. More than 90% of the initial ^{14}C in Av2 was recovered as modified Glu 112, and no additional residues were found to contain ^{14}C. Hence, the residue specificity, at least as far as the Av2 portion of the cross-linking reaction is concerned, is independent of the attacking nucleophile.

Unlike the more general use of carbodiimides to modify carboxyl groups in proteins, the cross-linking reaction and the glycinamide incorporation were effective at low concentrations of reactants. The rate and amount of glycinamide incorporated were investigated in detail for two concentrations of glycinamide, 4 and 25 mM (data not shown). At both concentrations, the rate curves could be fit with a model of a rapid first-order rate of incorporation of a single glycinamide, followed with a slower rate (ca. 0.1% of the first rate) corresponding to the incorporation of more than eight glycinamide residues per subunit. Both the shape of the curves and the concentration dependence indicate a first-order nucleophilic attack by glycinamide on the carbodiimide-activated carboxyl. In contrast, the EDC concentration dependencies of the cross-linking and glycinamide incorporation rates were unaltered in the range of 5−20 mM EDC.

The pocket of carboxylate groups around Glu 112 (Figures 2A and 4) and the specificity of the site of the reaction at Glu 112 for both glycinamide and cross-linking suggest that the EDC might behave as an active site-directed reagent. The lack of EDC concentration dependence is consistent with

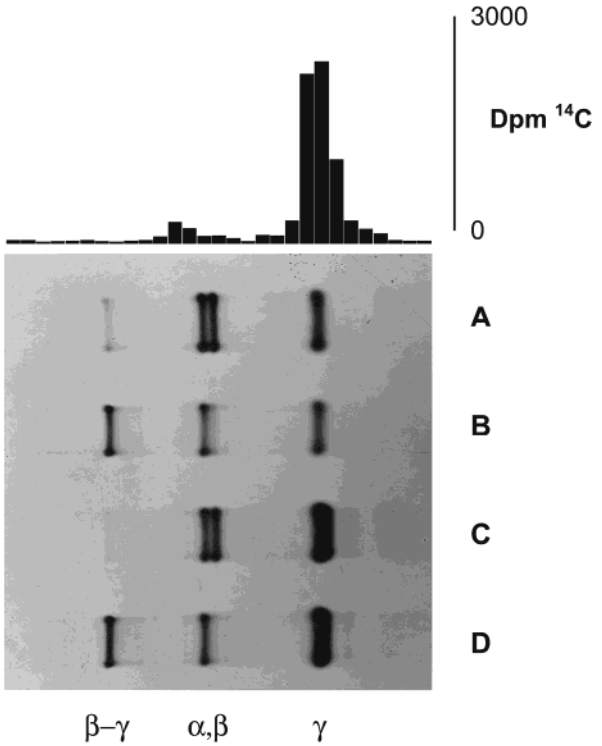

FIGURE 5: Inhibition of EDC-mediated cross-linking of Av1 and Av2 by glycinamide as assessed by SDS−acrylamide gel electrophoresis. For lanes A and B, Av1 (95 μg) and Av2 (165 μg) were reacted with 12.5 mM EDC for 15 min in 200 μL of pH 8.0 HEPES buffer containing 5 mM sodium dithionite. For panel A, 25 mM [2-^{14}C]glycinamide was included. The reactions were stopped by adding SDS and 2-mercaptoethanol. For lanes C and D, Av1 (950 μg) or Av2 (1650 μg) was reacted separately with 12.5 mM EDC and 25 mM glycinamide for 15 min in 1.0 mL of pH 8.0 HEPES buffer containing 5 mM sodium dithionite. The proteins were rapidly removed from the reaction mixture by filtration on Sephadex G-25 (1.2 cm × 20 cm column) in pH 8.0 HEPES buffer containing 5 mM sodium dithionite. Each reisolated protein was incubated with EDC and fresh, unreacted complementary component protein under the conditions described above. Lane C contained Av2 modified by EDC and glycinamide with fresh Av1. Lane D contained Av1 with fresh Av2. Lane A was cut into 30 strips (5 mm). Each strip was digested with 30% H_2O_2 overnight and the radioactivity determined by scintillation counting. A plot of the radioactivity is shown above the gel. The small amount of radioactivity seen at a MW of ~65000 is likely due to incorporation into Av2 having an internal cross-link (J. K. Magnuson and J. B. Howard, unpublished results): $\beta-\gamma$, cross-linked Av1 and Av2 subunits; α,β, two subunits of Av1; and γ, γ-subunits of Av2.

a binding step prior to reacting with Glu 112, a characteristic of an active site-directed agent. It should be noted that the structure of EDC has a cationic group [(dimethylamino)-propyl group] that could be binding in the cation binding pocket of Av2. To test this, Av2 was reacted in both cross-linking and glycinamide incorporation with two other peptide bond-mediating reagents, Woodward's Reagent K, which has a negatively charged sulfonic acid functional side chain, and diisopropylcarbodimide, which is an analogue of EDC without a charged side chain. Neither reagent, even at 100 mM, resulted in specific cross-linking or glycinamide incorporation, although both produced nonspecific cross-linking, mainly in the form of high-molecular weight aggregates. These results are consistent with the hypothesis that EDC serves as a site-directed reagent in Av2.

EDC-mediated cross-linking of the components leads to the rapid loss of activity in the nitrogenase reduction of substrates (*19*), while the addition of glycinamide to the cross-linking reaction results in nearly full protection against this inactivation (results not shown). The individual proteins likewise retained their activity when reacted with EDC and glycinamide. Thus, glycinamide modification of Av2 has little effect on the activity of the Fe-protein for substrate reduction. A more detailed kinetic analysis found that modified Av2 exhibits ~85% of the specific activity of native Av2 and requires an ~2-fold increase in Av2 concentration for half-saturation of Av1. Together, these results strongly indicate that formation of a nondissociating, cross-linked complex is responsible for the enzymatic inactivation, and it is neither the EDC reaction itself nor, most importantly, the modification of Av2 Glu 112 that leads to inactivation.

Not withstanding the small number of interactions between Av1 and Av2 in the structure of the cross-linked complex, there are several lines of experimental evidence that support the mechanistic relevance of these interactions. As noted in the original characterization of this complex (*18*, *19*), the cross-linking reaction is dependent upon the protein concentration, the ratio of the component proteins, and the salt concentration in a way similar to that observed for substrate reduction. The exquisite selectivity of the cross-linking reaction for Glu 112 and Lys β400, but none of the potentially reactive neighboring groups, is an indication that the cross-linking takes place in a specific complex. The FeMo-cofactor deficient state of Av1, a form of Av1 that requires Av2 complex formation during cofactor insertion, can also cross-link with Av2 (*29*), and the recently determined structure of an FeMo-cofactor deficient form of Av1 (*30*) confirms that the site of Av2 cross-linking with native Av1 is still intact in this species. Also arguing against a nonspecific, electrostatically stabilized interaction between the nitrogenase proteins is the observation that other proteins with basic charged patches, such as lysozyme and cytochrome *c*, do not cross-link to Av2. Furthermore, Av2 is a selective partner with respect to both conformational integrity and the activation of Glu 112. Altered forms of Av2 with substitutions at Arg 100 are substantially slowed in cross-linking to Av1 (*31*), even though Arg 100 is not directly in contact with Av1 in the cross-linked structure. Interestingly, these Arg 100 mutants seem to remain fully reactive for glycinamide incorporation. Other mutant forms of Av2, where the amino acid substitution is located in the interior of the molecule, have normal reactivity in cross-linking with Av1 (*32*, *33*).

While the pathway for the interconversion of the putative pre-cross-linking complex of the nitrogenase proteins, as represented by the EDC-trapped species, and the likely electron transfer complex, as exemplified by the ADP-AlF_4^--stabilized complex, is not known, a possible scenario can be constructed from the following considerations. By analogy to the structurally homologous G-protein family (*12*), the pre- and post-ATP hydrolysis complexes of nitrogenase will undoubtedly differ, at least in detail, from the ADP-AlF_4^--stabilized complex. In contrast to the MoFe-protein, the Fe-protein exhibits considerable structural variability and flexibility (*17*, *34*, *35*), including the Av2 dimers observed here. As a first approximation, it is reasonable to consider the MoFe-protein as a fixed template, with the Fe-protein undergoing a sequence of conformational changes while in

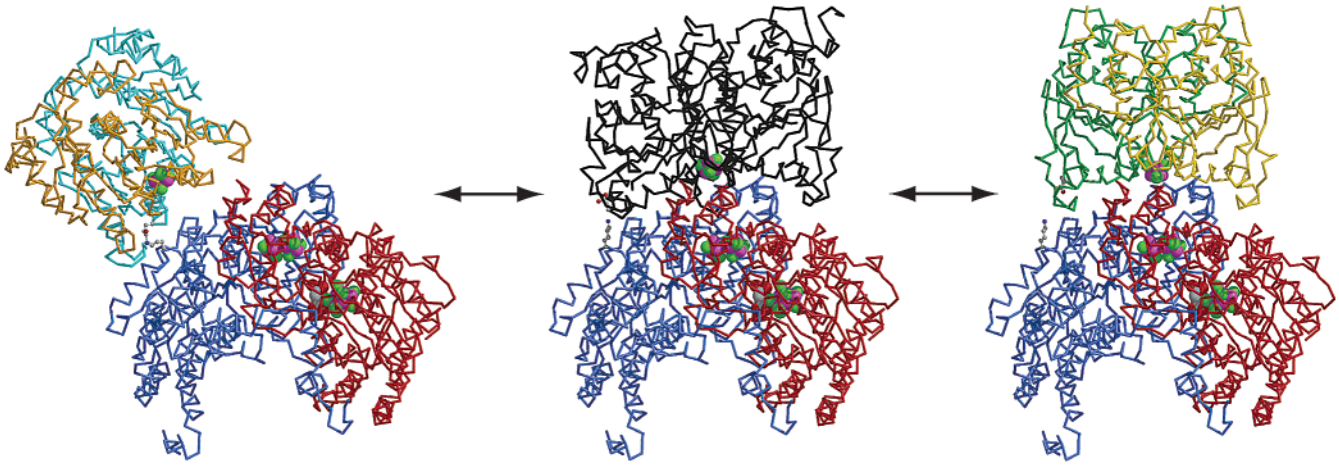

FIGURE 6: Schematic of the hypothetical transition from an initial encounter complex between Av1 and Av2, as modeled in the cross-linked complex (left), to the electron transfer competent state reflected in the ADP-AlF_4^--stabilized complex (right). The middle complex (see also Figure 3B) illustrates a proposed intermediate complex generated by superimposing the native, nucleotide-free Av2 (black) onto the Av2 subunit of the ADP-AlF_4^--stabilized complex interacting with the Av1 α-subunit. The interconversion to this intermediate state could involve a "rocking motion" with a pivot near Asp 69 that swings Av2 from the position observed in the cross-linked complex to that in the ADP-AlF_4^--stabilized complex, while keeping Glu 112 and Lys β400 in proximity. The double-sided arrows indicate that these transitions may also be relevant to dissociation of the electron transfer competent complex. The view and coloring scheme are as in Figure 1, with the cross-linked residues depicted as ball-and-stick models. This figure was prepared with Molscript (*39*) and Raster3D (*40*).

contact with different regions of the MoFe-protein surface.

With these guidelines, the relationship between the EDC-cross-linked complex and the ADP-AlF_4^--stabilized complex can be considered. Analysis of the ADP-AlF_4^--stabilized complex indicates that chemical cross-linking between Glu 112 and Lys β400 is unlikely to occur in that complex. Although the γ-carboxyl of Glu 112 is open to approach by EDC and is poised above the Nζ-amino of Lys β400, they are >10 Å apart, a separation much too great for formation of an isopeptide bond, and indeed, we do not observe EDC-mediated cross-linking after the ADP-AlF_4^--stabilized complex has been formed (data not presented). For the cross-linking, the Av1 β-subunit and Av2 must be in closer contact. One such model is to substitute the Av2−ADP-AlF_4^- conformation with the more open, nucleotide-free conformation observed in the native Av2 structure. When native Av2 is superimposed on the structure of Av2 in the ADP-AlF_4^--stabilized complex, using the subunit most associated with the Av1 α-subunit (the subunit *away* from the cross-linking side), the γ-carboxyl of Glu 112 is now within a distance appropriate for isopeptide formation with the Nζ-amino of Lys β400. The fixing of the interactions between one Av2 subunit and the Av1 α-subunit reflects the conservation of these interactions in the ADP-AlF_4^-- and L127Δ Av2-stabilized complexes (*11*, *17*), while the interactions on the β-subunit are somewhat more variable. An illustration of this hypothetical species is provided in Figures 3B and 6. As built, such a complex cannot be fully correct as there are several unacceptable clashes at the interface; indeed, it is the conformational changes in the Av2−ADP-AlF_4^- complex that in part relieve these clashes. These binding modes do, however, suggest a plausible model for the "glide path" approach of Av2, initially interacting on the β-subunit side of Av1, to the ultimately productive electron transfer intermediate approximated by the ADP-AlF_4^--stabilized complex.

The details of the conversion between the putative initial encounter complex reflected in the cross-linked species and the ADP-AlF_4^--stabilized complex remain enigmatic. MgATP is critical for this transition; the cross-linking reaction is the presence of nucleotide (*18*), suggesting the rearrangement of Av2 from the encounter complex to the electron transfer competent species must require nucleotide. In view of the sensitivity observed in the relative orientations of the Fe-protein subunits to the binding of nucleotide and MoFe-protein (*17*, *34*, *35*), it is likely that MgATP promotes this rearrangement through stabilization of an Fe-protein conformation, perhaps more open than the wild type, that can bridge the Av2 binding sites observed in the cross-linked and ADP-AlF_4^--stabilized complexes. As also evidenced by the structure of the cross-linked complex, significant flexibility in the interaction between the component proteins should be accommodated in the initial complex, as there appear to be few constraints to rotation about the isopeptide linkage. Thus, rotation of the bound Av2, as seen in the cross-linked complex, toward the Av2−ADP-AlF_4^- binding site seems plausible. This interaction could involve a "pivoting" function involving the region of Av2 near Asp 69, since it is positioned near Lys β400 in both complexes, and furthermore, it is located in one of the most conformationally variable loops in the Fe-protein (*34*). Changes in residues 59−67 near this region of Av2 have also been found to influence the association behavior with the MoFe-protein (*36*). Similar considerations may be relevant as well to the dissociation of the Av1−Av2 complex following electron transfer (Figure 6).

The isopeptide clearly prevents Av2 from progressing to the electron transfer conformation exhibited by the ADP-AlF_4^--stabilized complex. It is this restriction that can explain why the cross-linked nitrogenase complex is enzymatically inactive. Indeed, a recent analysis provides a compelling demonstration of the effect of the length of the cross-linker on the kinetics of interprotein electron transfer (*37*). When two azurin molecules are cross-linked with a long linker connecting the surfaces believed to associate during the electron self-exchange reaction, the resulting dimer exhibits efficient interprotein electron transfer. In contrast, the use of a shorter cross-linker leads to greatly reduced rates,

presumably due to restrictions in the relative positioning of the partner proteins in the complex. This latter situation may be relevant to the behavior of the cross-linked nitrogenase complex, and emphasizes that while cross-linked complexes may be compromised with respect to electron transfer capabilities, with appropriate characterization, these species can serve to identify the interface surface between interacting proteins.

ACKNOWLEDGMENT

We thank A. Deacon and the staff at the Stanford Synchrotron Radiation Laboratory for assistance with data collection.

REFERENCES

1. Burgess, B. K., and Lowe, D. J. (1996) *Chem. Rev. 96*, 2983−3011.
2. Howard, J. B., and Rees, D. C. (1996) *Chem. Rev. 96*, 2965−2982.
3. Seefeldt, L. C., and Dean, D. R. (1997) *Acc. Chem. Res. 30*, 260−266.
4. Smith, B. E. (1999) *Adv. Inorg. Chem. 47*, 159−218.
5. Rees, D. C., and Howard, J. B. (2000) *Curr. Opin. Chem. Biol. 4*, 559−566.
6. Howard, J. B., and Rees, D. C. (1994) *Annu. Rev. Biochem. 63*, 235−264.
7. Hageman, R. V., and Burris, R. H. (1978) *Proc. Natl. Acad. Sci. U.S.A. 75*, 2699−2702.
8. Thorneley, R. N. F., and Lowe, D. J. (1985) in *Molybdenum Enzymes* (Spiro, T. G., Ed.) pp 221−284, John Wiley & Sons, New York.
9. Renner, K. A., and Howard, J. B. (1996) *Biochemistry 35*, 5353−5358.
10. Duyvis, M. G., Wassink, H., and Haaker, H. (1996) *FEBS Lett. 380*, 233−236.
11. Schindelin, H., Kisker, C., Schlessman, J. L., Howard, J. B., and Rees, D. C. (1997) *Nature 387*, 370−376.
12. Vetter, I. R., and Wittinghofer, A. (2001) *Science 294*, 1299−1304.
13. Wolle, D., Dean, D. R., and Howard, J. B. (1992) *Science 258*, 992−995.
14. Georgiadis, M. M., Komiya, H., Chakrabarti, P., Woo, D., Kornuc, J. J., and Rees, D. C. (1992) *Science 257*, 1653−1659.
15. Thorneley, R. N. F. (1992) *Philos. Trans. R. Soc. London, Ser. B 336*, 73−82.
16. Ryle, M. J., and Seefeldt, L. C. (1996) *Biochemistry 35*, 4766−4775.
17. Chiu, H.-J., Peters, J. W., Lanzilotta, W. N., Ryle, M. J., Seefeldt, L. C., Howard, J. B., and Rees, D. C. (2001) *Biochemistry 40*, 641−650.
18. Willing, A. H., Georgiadis, M. M., Rees, D. C., and Howard, J. B. (1989) *J. Biol. Chem. 264*, 8499−8503.
19. Willing, A., and Howard, J. B. (1990) *J. Biol. Chem. 265*, 6596−6599.
20. Wolle, D., Kim, C., Dean, D., and Howard, J. B. (1992) *J. Biol. Chem. 267*, 3667−3673.
21. Hausinger, R. P., and Howard, J. B. (1983) *J. Biol. Chem. 258*, 13486−13492.
22. Otwinowski, Z. (1991) in *Isomorphous Replacement and Anomalous Scattering* (Wolf, W., Evans, P., and Leslie, A., Eds.) pp 80−86, SERC Daresbury Laboratory, Warrington, U.K.
23. Navaza, J. (1994) *Acta Crystallogr. A50*, 157−163.
24. Brünger, A. T., Adams, P. D., Clore, G. M., DeLano, W. L., Gros, P., Grosse-Kunstleve, R. W., Jiang, J.-S., Kuszewski, J., Nilges, M., Pannu, N. S., Read, R. J., Rice, L. M., Simonson, T., and Warren, G. L. (1998) *Acta Crystallogr. D54*, 905−921.
25. Peters, J. W., Stowell, M. H. B., Soltis, S. M., Finnegan, M. G., Johnson, M. K., and Rees, D. C. (1997) *Biochemistry 36*, 1181−1187.
26. Oliver, M. E., and Hales, B. J. (1993) *Biochemistry 32*, 6058−6064.
27. Janin, J. (1997) *Nat. Struct. Biol. 4*, 973−974.
28. Hoare, D. G., and Koshland, D. E. (1967) *J. Biol. Chem. 242*, 2447−2453.
29. Magnuson, J. K., Paustian, T. D., Shah, V. K., Dean, D. R., Roberts, G. P., Rees, D. C., and Howard, J. B. (1997) *Tetrahedron 53*, 11971−11984.
30. Schmid, B., Ribbe, M. W., Einsle, O., Yoshida, M., Thomas, L. M., Dean, D. R., Rees, D. C., and Burgess, B. K. (2002) *Science 296*, 352−356.
31. Howard, J. B. (1993) in *Molybdenum Enzymes, Cofactors and Model Systems* (Stiefel, E. I., Coucouvanis, D., and Newton, W. E., Eds.) ACS Symposium Series 535, pp 271−289, American Chemical Society, Washington, DC.
32. Seefeldt, L. C., Morgan, T. V., Dean, D. R., and Mortenson, L. E. (1992) *J. Biol. Chem. 267*, 6680−6688.
33. Gavini, N., and Burgess, B. K. (1992) *J. Biol. Chem. 267*, 21179−21186.
34. Schlessman, J. L., Woo, D., Joshua-Tor, L., Howard, J. B., and Rees, D. C. (1998) *J. Mol. Biol. 280*, 669−685.
35. Jang, S. B., Seefeldt, L. C., and Peters, J. W. (2000) *Biochemistry 39*, 14745−14752.
36. Peters, J. W., Fisher, K., and Dean, D. R. (1994) *J. Biol. Chem. 269*, 28076−28083.
37. van Amsterdam, I. M. C., Ubbink, M., Einsle, O., Messerschmidt, A., Merli, A., Cavazzini, D., Rossi, G. L., and Canters, G. W. (2002) *Nat. Struct. Biol. 9*, 48−52.
38. Laskowski, R. A., MacArthur, M. W., Moss, D. S., and Thornton, J. M. (1993) *J. Appl. Crystallogr. 26*, 283−291.
39. Kraulis, P. J. (1991) *J. Appl. Crystallogr. 24*, 946−950.
40. Merritt, E. A., and Murphy, M. E. P. (1994) *Acta Crystallogr. D50*, 869−873.
41. Honig, B., and Nicholls, A. (1995) *Science 268*, 1144−1149.
42. Sanner, M. F., Olson, A. J., and Spehner, J.-C. (1996) *Biopolymers 38*, 305−320.

BI026642B